

SPE 80925

## Single-Phase Model for ESP's Head Performance

Datong Sun and Mauricio Prado, SPE, the University of Tulsa

Copyright 2003, Society of Petroleum Engineers Inc.

This paper was prepared for presentation at the SPE Production and Operations Symposium held in Oklahoma City, Oklahoma, U.S.A., 22–25 March 2003.

This paper was selected for presentation by an SPE Program Committee following review of information contained in an abstract submitted by the author(s). Contents of the paper, as presented, have not been reviewed by the Society of Petroleum Engineers and are subject to correction by the author(s). The material, as presented, does not necessarily reflect any position of the Society of Petroleum Engineers, its officers, or members. Papers presented at SPE meetings are subject to publication review by Editorial Committees of the Society of Petroleum Engineers. Electronic reproduction, distribution, or storage of any part of this paper for commercial purposes without the written consent of the Society of Petroleum Engineers is prohibited. Permission to reproduce in print is restricted to an abstract of not more than 300 words; illustrations may not be copied. The abstract must contain conspicuous acknowledgment of where and by whom the paper was presented. Write Librarian, SPE, P.O. Box 833836, Richardson, TX 75083-3836 U.S.A., fax 01-972-952-9435.

### Abstract

This paper presents a new incompressible single-phase model for ESP's head performance. Sachdeva (1988) and Cooper (1966) developed models for ESP channels [1, 2] and for inducers [3], respectively. The model presented in this paper is based on one-dimensional approximation along an ESP channel. The new derived pressure ODE (Ordinary Differential Equation) for frictionless incompressible flow is consistent with the pump Euler equation. New models for pump frictional and shock losses have been proposed. Finally, a comparison between the predicted pump performance and the pump performances from Affinity Law for different rotational speeds is presented. The single-phase model can predict ESP performance under different fluid viscosities and also is the basis of gas-liquid model for ESP's head performance.

### Introduction

This paper presents the new single-phase model developed for the prediction of an ESP's performance. The correct ESP head performance is critical for the appropriate design, simulation and troubleshooting of an ESP installation. The model consists of the mass and momentum equations, based on the streamline approach or one-dimensional assumption. In the momentum equations, the calculation of the friction factor proposed by Sachdeva, is improved by incorporating the channel curvature, channel rotation, and channel cross-section effects. A new shock loss model including rotational speeds has been proposed. The new single-phase model is capable of predicting the pump performance for different rotational speeds and for different viscosities.

### Literature Review

Sachdeva (1988, 1994) derived the frictionless pressure ODE under incompressible single-phase flow as follows,

$$\frac{1}{\rho_l} \frac{dp}{dr} = \omega^2 r - \frac{1}{2} \frac{d}{dr} (V_r^2), \quad (1)$$

where  $p$  is pressure,  $\omega$  is angular velocity,  $r$  is radius along the channel,  $\rho_l$  is liquid density, and  $V_r$  is the radial component of absolute velocity.

Sachdeva's previous equation needs to be extended for any blade angle in an ESP.

The frictionless pressure ODE given by Cooper (1966) for an inducer [3],

$$\frac{dp}{\rho_l} = \omega^2 r dr - W dW, \quad (2)$$

where  $W$  is the relative velocity.

Different investigators such as Sachdeva and Cooper superimposed frictional losses into their frictionless pressure ODE.

The friction factor in Sachdeva's frictional loss model considers the effects of curvature for the diffuser and both curvature and rotational speed for the impeller.

Sachdeva's approach for friction factor calculation is very important to model pump performance. His approach assumed smooth surface and turbulent flow regime inside ESP channels.

### Mass Balance Equation

The derivation of the one-dimensional mass balance equation [4] yields the following expression along the channel in an impeller or diffuser.

$$\frac{\partial}{\partial t} (\rho_l) + \frac{1}{r \sin \beta} \frac{\partial}{\partial s} (r \rho_l W \sin \beta) = 0, \quad (3)$$

where  $\beta$  is the geometric blade angle as shown in Fig.1,  $s$  is the streamline coordinate, which is the distance between the entrance to any location along the channel, and  $t$  is time. The streamline in this one-dimensional model is at the center of the channel and has the same shape as its two blades.

For steady-state incompressible liquid flow along the ESP channel, the relative velocity  $W$  can be expressed as,

$$W = \frac{Q_l}{2\pi r H \sin \beta}, \quad (4)$$

where  $Q_l$  is the liquid flow rate and  $H$  is the channel height.

## Pump Head Equation

The head developed by each pump stage includes two parts: impeller head and diffuser head. The equations for the frictionless case will be presented first. Details of the derivation of the frictionless pressure and head equation can be found in Sun (2002) [4]. Later in this section, the final form of the model, including friction, will be presented.

**Frictionless Pressure and Head Equation.** If the fluid friction is neglected, the pressure ODE along the channel at radius  $r$  is,

$$\left. \frac{dp}{dr} \right|_{streamline} = \left[ -\rho_l \frac{\partial W}{\partial t} \frac{ds}{dr} + \rho_l \omega^2 r \right] , \quad (5)$$

$$= \left[ -\frac{\rho_l}{2} \frac{dW^2}{dr} + \rho_l g_s \frac{ds}{dr} \right]_{streamline}$$

where  $g_s$  is the gravitational acceleration in the streamline direction, subscript  $s$  signifies the streamline.

The steady-state frictionless pressure ODE along an ESP channel can be simplified as,

$$dp = (\rho_l \omega^2 r) dr - \rho_l \frac{d(W^2)}{2} - \rho_l g_s ds, \quad (6)$$

After integration of the pressure ODE along the streamline, the pressure increment in the impeller can be expressed as,

$$p_2 - p_1 = \left( \frac{\omega^2 r_2^2 - \omega^2 r_1^2}{2} + \frac{W_1^2 - W_2^2}{2} + g(z_{v1} - z_{v2}) \right) \rho_l, \quad (7)$$

where subscript  $l$  indicates the entrance of an impeller or a diffuser,  $z_{v1}, z_{v2}$  are the vertical components of the  $z$  value at the impeller entrance and discharge, respectively.

By definition, impeller head can also be expressed as,

$$H_{impeller} = \frac{p_2 - p_1}{\rho_l g} + \frac{V_2^2 - V_1^2}{2g} + (z_{v2} - z_{v1}), \quad (8)$$

where  $V$  is the absolute velocity.

Combining the previous two equations, the impeller head becomes,

$$H_{impeller} = \frac{V_2^2 - V_1^2}{2g} + \frac{U_2^2 - U_1^2}{2g} + \frac{W_1^2 - W_2^2}{2g}, \quad (9)$$

where  $U$  is the peripheral velocity, which can be expressed as,

$$U = \omega r. \quad (10)$$

The velocity relationship along a radial impeller channel can be illustrated as Fig. 1.

Since the frictionless diffuser head is zero, the frictionless pump head for a stage is equal to the impeller head,

$$H_{stage} = \frac{V_2^2 - V_1^2}{2g} + \frac{U_2^2 - U_1^2}{2g} + \frac{W_1^2 - W_2^2}{2g}. \quad (11)$$

It is documented that the pump head derived from the new frictionless model for a stage is the same as the Euler head [5]. Therefore, the new frictionless pressure ODE is correct. The Euler pump head  $H_e$  is,

$$H_e = \frac{V_2^2 - V_1^2}{2g} + \frac{U_2^2 - U_1^2}{2g} + \frac{W_1^2 - W_2^2}{2g}. \quad (12)$$

Using the velocity relationships, the Euler head can also be expressed as,

$$H_e = \frac{U_2^2 - U_1^2}{g} - \frac{W_2 U_2 \cos \beta_2 - W_1 U_1 \cos \beta_1}{g}. \quad (13)$$

Finally, the Euler head  $H_e$  can be expressed as,

$$H_e = \frac{\omega^2}{g} (r_2^2 - r_1^2) - \frac{Q_l \omega}{2\pi g H} \left( \frac{1}{\tan \beta_2} - \frac{1}{\tan \beta_1} \right). \quad (14)$$

The gravitational term in equation (6) is small compared to the centrifugal force and can be neglected. The final frictionless pressure equation agrees with Eq. 2 presented by Cooper (1966) [3].

## Pressure and Head Equation Including Friction Losses.

When fluid friction is considered, the friction loss term can be superimposed onto the pressure frictionless ODE equation. The pressure distribution ODE at the radial position  $r$  along an ESP channel then becomes:

$$dp = \rho_l \omega^2 r dr - \rho_l \frac{dW^2}{2} + \left( \frac{dp}{dr} \right)_f dr - \rho_l g_s ds, \quad (15)$$

where  $\left( \frac{dp}{dr} \right)_f$  is the pressure radial gradient due to fluid

friction, which can be related to a pressure gradient  $\left( \frac{dp}{ds} \right)_f$

along the channel length position  $s$  as,

$$\left( \frac{dp}{dr} \right)_f = \left( \frac{dp}{ds} \right)_f \frac{ds}{dr}, \quad (16)$$

the relationship between  $s$  and  $r$  can be expressed as,

$$\frac{ds}{dr} = \frac{j}{\sin \beta_h \cos \gamma}, \quad (17)$$

and  $j=1$  for impeller and  $j=-1$  for diffuser. If the channel has a hydraulic diameter  $d_H$  and the fluid is moving with a relative

velocity  $W$  to the channel, the term  $\left( \frac{dp}{ds} \right)_f$  is given by,

$$\left( \frac{dp}{ds} \right)_f = -f \frac{\rho}{d_H} \frac{W^2}{2}, \quad (18)$$

where  $f$  is a friction factor. Expression for the friction factor  $f$  will be discussed in a later section.

Equation (15) is valid for impeller ( $\omega = \omega_{impeller}$ ) and diffuser ( $\omega = 0$ ), where  $\omega_{impeller}$  is the impeller angular velocity.

The pump head per stage without shock losses can be calculated using the pressure increment between the impeller eye and the next stage of the impeller eye, as follows,

$$H_{stage} = \frac{P_{next\_Eye} - P_{Eye}}{\rho_l g}, \quad (19)$$

where  $P_{Eye}$  is the impeller eye pressure of the stage intake,

$P_{next\_Eye}$  is the impeller eye pressure of the next stage.

The shock losses in the single-phase condition can be estimated with Pfeiderer and Peterman's (1986) formula [6]. In this study, the shock losses for water is calculated using the head difference, as shown in Fig.2, between the head performance for water from the frictional model and the actual pump performance from the manufacturer. The shock losses for water at certain rotational speed,  $\Delta H_{shock,water,base}$ , can be regressed as a quadratic equation as follows,

$$\Delta H_{shock,water,base} = a_{shock,base} Q_l^2 + b_{shock,base} Q_l + c_{shock,base}, \quad (20)$$

where the three coefficients  $a_{shock,base}$ ,  $b_{shock,base}$ ,  $c_{shock,base}$  are corresponding to the water shock losses at certain rotational speed, called base rotational speed.

In this study, the shock losses for different rotational speeds is assumed to follow the affinity laws. Then the head shock loss for any single-phase liquid property under any rotational speed  $\omega_{impeller}$  is proposed as,

$$\Delta H_{shock,l} = \left[ \frac{\omega_{impeller}}{\omega_{impeller,base}} \right]^2 \left[ a_{shock,base} \left( Q_l \frac{\omega_{impeller,base}}{\omega_{impeller}} \right)^2 + b_{shock,base} \left( Q_l \frac{\omega_{impeller,base}}{\omega_{impeller}} \right) + c_{shock,base} \right]. \quad (21)$$

Accordingly, the pressure shock losses can be proposed as,

$$\Delta p_{shock,l} = \rho_l g \left[ a_{shock,base} Q_l^2 + b_{shock,base} \left( Q_l \frac{\omega_{impeller}}{\omega_{impeller,base}} \right) + c_{shock,base} \left( \frac{\omega_{impeller}}{\omega_{impeller,base}} \right)^2 \right]. \quad (22)$$

Finally, the pump pressure increment and pump head per stage will be as follows, respectively,

$$\Delta p_{stage} = P_{next\_Eye} - P_{Eye} - \Delta p_{shock,tp}, \quad (23)$$

and,

$$H_{stage} = \frac{\Delta p_{stage}}{\rho_l g}. \quad (24)$$

### Calculation of Friction Factor

To calculate the friction factor, the hydraulic diameter is needed and is related with the cross-section geometry. An ESP channel has a near rectangular cross-section with a channel width  $a$  and a channel height  $b$ , as shown in Fig.3. They can be obtained from the geometric relationship,

$$a = \frac{2\pi r}{n} \sin \beta, \quad (25)$$

$$b = H, \quad (26)$$

where  $n$  is the number of impeller blades or diffuser blades.

The hydraulic diameter,  $d_H$ , can be expressed as,

$$d_H = \frac{2ab}{a+b}. \quad (27)$$

**Reynolds Number.** The friction factor depends on whether the flow regime occurring in the channel is laminar or turbulent. The determination of the flow regime depends on the Reynolds number  $N_{Re}$ , which is related to the relative velocity  $W$  along ESP channels as,

$$N_{Re} = \frac{d_H W \rho_l}{\mu_l}, \quad (28)$$

where  $\mu_l$  is liquid viscosity.

Here, the friction factor for circular, straight stationary pipes will be presented, since it will be used as the starting point for inclusion of the mentioned characteristics of ESP channels.

**Friction Factor for Straight Stationary Pipes with Circular Cross Sections.** For flow inside a straight stationary pipe with circular cross section, namely, for flow inside a normal pipe, the transition between laminar and turbulent flow occurs at a critical Reynolds number as follows,

$$(N_{Re})_{crit\_normal} = 2300. \quad (29)$$

In the rest of this document, one can adopt the following nomenclature for friction factor,

$$f_{shape, curvature, movement}$$

The first subscript, "shape", indicates the shape of the cross-section in the channel; the second subscript, "curvature", indicates if the channel is curved or straight; the third subscript, "movement", indicates if the channel is stationary or rotating.

The friction factor for laminar flow in a circular, straight, stationary pipe is given by,

$$f_{\text{circular, straight, stationary}} = \frac{64}{N_{\text{Re}}} \quad (30)$$

The friction factor for turbulent flow in a circular, straight, stationary pipe is given by Churchill (1977) [7] as follows,

$$f_{\text{circular, straight, stationary}} = \left[ 8 \left[ 2.457 \ln \frac{1}{\left( \frac{7}{N_{\text{Re}}} \right)^{0.9} + 0.27 \left( \frac{\varepsilon}{d_H} \right)} \right] \right]^{-2}, \quad (31)$$

where  $\varepsilon$  is the absolute roughness of the channel.

**Friction factor effects.** The friction factor used in a straight, stationary pipe with a circular cross section is not applicable to ESP impeller and diffuser channels. An ESP channel has a rectangular cross-section, is curved and the impeller rotates during operation. The flow inside this geometry is very different from the one encountered inside straight, stationary pipes with circular cross-sections. The presence of secondary flows inside the impeller and diffuser channels must be considered as pointed out by Schlichting (1955) [8] and Ito (1971) [9].

Several investigators have studied the effects of channel curvature, cross-section shape, and rotational speed on the critical Reynolds number and on the friction factor. Unfortunately, though, the effect of each of these factors was studied independently of each other.

Sachdeva (1988, 1994) incorporated the one or two effects together for an ESP diffuser or impeller, which is very important for the friction factor calculation. In this study, the modified critical Reynolds Number and friction factor corrections presented in the later sections are an approximation of what occurs in an ESP channel when more than one of those factors is actually influencing the flow simultaneously.

Here, each independent effect is presented first.

**Cross Section Shape Effect.** Since only the shape effect is being considered, the flow regime can be determined using the Reynolds number for cross-section effect. The works of Shah (1978) [10] and Jones (1976) [11] will be used to calculate the shape effect on the friction factor for laminar and turbulent flow, respectively.

**Critical Reynolds number.** The critical Reynolds Number for flow regime transition due to shape effect is:

$$(N_{\text{Re}})_{\text{crit\_rectangular}} = 2300. \quad (32)$$

**Laminar Flow.** If  $N_{\text{Re},l} \leq (N_{\text{Re}})_{\text{crit\_rectangular}}$ , then laminar flow occurs.

The effect of the rectangular cross-section shape on the friction factor for straight, stationary pipes in laminar flow has been studied by Shah (1978).

The “laminar equivalent diameter”  $d_{eq}$ , which is defined based on the work of Cornish (1928) [12], can be used to calculate the friction factor under laminar flow.

$$d_{eq} = \left[ \frac{2}{3} + \frac{11}{24} l (2-l) \right] d_H, \quad (33)$$

where  $l$  is the aspect ratio of the rectangular cross section for liquid defined as,

$$l = \frac{\min(a, b)}{\max(a, b)}, \quad (34)$$

The corresponding equivalent Reynolds number  $N_{\text{Re}_{eq}}$  is:

$$N_{\text{Re}_{eq}} = \frac{d_{eq} W \rho_l}{\mu_l}. \quad (35)$$

For fluid flowing in a rectangular cross-section, straight, stationary pipe under a laminar flow, the friction factor as presented by Shah (1978) is,

$$f_{\text{rectangular, straight, stationary}} = \frac{64}{N_{\text{Re}_{eq}}}. \quad (36)$$

The multiplication factor  $F_{\text{rectangular}}$  under laminar flow for a diffuser or an impeller with a rectangular cross section can finally be written as,

$$\begin{aligned} F_{\text{rectangular}} &= \frac{f_{\text{rectangular, straight, stationary}}}{f_{\text{circular, straight, stationary}}} \\ &= \frac{1}{\frac{2}{3} + \frac{11}{24} l (2-l)}. \end{aligned} \quad (37)$$

**Turbulent Flow.** If  $N_{\text{Re}} > (N_{\text{Re}})_{\text{crit\_rectangular}}$ , then turbulent flow occurs.

The effect of the rectangular cross-section shape on the friction factor for straight, stationary pipes in turbulent flow was studied by Jones (1976) [11].

The author suggested that the “laminar equivalent diameter”,  $d_{eq}$ , also be used to calculate the friction factor under turbulent flow.

The friction factor for turbulent flow in a smooth, straight, stationary pipe with rectangular cross-section can be expressed by the Blasius equation based on the equivalent Reynolds number.

$$f_{\text{rectangular, straight, stationary}} = 0.316 \times N_{\text{Re}_{eq}}^{-0.25}. \quad (38)$$

One can then obtain the multiplication factor,  $F_{\text{rectangular}}$ , under turbulent flow for a diffuser or impeller with a rectangular cross section as:

$$F_{\text{rectangular}} = \frac{f_{\text{rectangular, straight, stationary}}}{f_{\text{circular, straight, stationary}}} = 1$$

$$= \left[ \frac{2}{3} + \frac{11}{24} l (2-l) \right]^{0.25} \quad (39)$$

**Pipe Curvature Effect.** The pipe curvature effect on the friction factor for circular cross-section, stationary pipes has been studied by Ito (1959) [13]. The pipe curvature effect changes the criteria for determination of the flow regime and calculation of friction factor.

Ito (1959) presented criteria to determine the importance of the curvature. If the radius of curvature is large, compared to the hydraulic radius  $r_H$ , then the channel can be treated as a straight pipe. If the radius of curvature is small, in comparison to the hydraulic radius, the author presented a new critical Reynolds number for the flow regime transition and a new expression for calculating the friction factors.

**Critical Reynolds Number.** The transition from laminar to turbulent flow then occurs at a critical Reynolds number,  $(N_{\text{Re}})_{\text{crit\_curved}}$ , which is a function of the channel radius of curvature,  $R_c$ , and the hydraulic radius,  $r_H$ , as follows,

$$(N_{\text{Re}})_{\text{crit\_curved}} = \begin{cases} 2 \times 10^4 \times \left( \frac{r_H}{R_c} \right)^{0.32} & \text{if } \frac{R_c}{r_H} < 860, \\ 2300 & \text{if } \frac{R_c}{r_H} \geq 860 \end{cases} \quad (40)$$

where  $r_H$  is the hydraulic radius based on the hydraulic diameter given by,

$$r_H = \frac{d_H}{2}. \quad (41)$$

**Laminar Flow Friction factor.** If the Reynolds number is less than the critical Reynolds number, namely,  $N_{\text{Re}} \leq (N_{\text{Re}})_{\text{crit\_curved}}$ , then the flow is laminar.

The laminar flow friction factor also depends on the ratio between the channel radius of curvature and the channel hydraulic radius.

#### (a) Straight Pipe Approach

If the ratio between the radius of curvature,  $R_c$ , and hydraulic radius,  $r_H$ , is equal or greater than 860, namely  $\left( \frac{R_c}{r_H} \geq 860 \right)$ , the pipe can be considered straight and the curvature multiplication factor,  $F_{\text{curved}}$ , is,

$$F_{\text{curved}} = \frac{f_{\text{circular, curved, stationary}}}{f_{\text{circular, straight, stationary}}} = 1. \quad (42)$$

#### (b) Curvature Effect Approach

If the ratio between the radius of curvature  $R_c$  and hydraulic radius  $r_H$  is less than 860, namely,  $\left( \frac{R_c}{r_H} < 860 \right)$ ,

curvature effects must be considered. The friction factor for laminar flow in curved pipes was obtained in this study by fitting White's (1929) empirical curve [13] sketched in Ito (1959), as follows,

$$f_{\text{circular, curved, stationary}} \sqrt{\frac{R_c}{r_H}} = 1.5 \left\{ \frac{\left[ N_{\text{Re}} \left( \frac{r_H}{R_c} \right)^{0.5} \right]^{-0.611}}{53} \right\} \quad (43)$$

Finally, a multiplication factor for the curvature effect  $F_{\text{curved}}$  is obtained as,

$$F_{\text{curved}} = \frac{f_{\text{circular, curved, stationary}}}{f_{\text{circular, straight, stationary}}} = 0.266 N_{\text{Re}}^{0.389} \left( \frac{r_H}{R_c} \right)^{0.1945} \quad (44)$$

**Turbulent Flow.** If the Reynolds number is larger than the critical Reynolds number, namely,  $N_{\text{Re}} > (N_{\text{Re}})_{\text{crit\_curved}}$ , then the flow is turbulent.

There are two sets of turbulent friction factor formulas available [13]. They were derived by using two different velocity profile assumptions. One is derived by using 1/7<sup>th</sup> – Power Velocity Distribution Law. The other is derived by using the logarithmic velocity distribution law. The assumption of 1/7<sup>th</sup> – Power Velocity Distribution Law is used in this study. Based on Ito's work, the following expression can be used for the multiplication factor for curvature effect in turbulent flow.

(a) If  $N_{\text{Re}} (r_H / R_c)^2 \geq 300$ , then,

$$F_{\text{curved}} = \frac{f_{\text{circular, curved, stationary}}}{f_{\text{circular, straight, stationary}}} = \left( N_{\text{Re}} \left( \frac{r_H}{R_c} \right)^2 \right)^{0.05} \quad (45)$$

(b) If  $300 > N_{\text{Re}} (r_H / R_c)^2 > 0.034$ , then,

$$F_{\text{curved}} = \frac{f_{\text{circular, curved, stationary}}}{f_{\text{circular, straight, stationary}}} = \quad (46)$$

$$= 0.092 \left[ N_{\text{Re}} \left( \frac{r_H}{R_c} \right)^2 \right]^{0.25} + 0.962$$

(c) If  $N_{\text{Re}} (r_H / R_c)^2 \leq 0.034$ , then,

$$F_{\text{curved}} = \frac{f_{\text{circular, curved, stationary}}}{f_{\text{circular, straight, stationary}}} = 1. \quad (47)$$

**Radius of Curvature.** The channel or streamline radius of curvature is an important parameter in calculating the friction factor for curvature effect.

In this study, a general equation for the three-dimensional channel radius of curvature [4] was derived, which is valid for radial and mixed pumps. The radius of curvature,  $R_c$ , for a point with coordinates  $x_1, y_1, z_1$  is:

$$R_c = \frac{1}{\sqrt{(x_c - x_1)^2 + (y_c - y_1)^2 + (z_c - z_1)^2}}, \quad (48)$$

where  $x_c, y_c, z_c$  are the center coordinates of the approximate circular interval of the channel, as shown in Fig. 4.

$$x_c = \frac{\det \begin{bmatrix} D_1 & A_{12} & A_{13} \\ D_2 & A_{22} & A_{23} \\ D_3 & A_{32} & A_{33} \end{bmatrix}}{\det \begin{bmatrix} A_{11} & A_{12} & A_{13} \\ A_{21} & A_{22} & A_{23} \\ A_{31} & A_{32} & A_{33} \end{bmatrix}}, \quad (49)$$

$$y_c = \frac{\det \begin{bmatrix} A_{11} & D_1 & A_{13} \\ A_{21} & D_2 & A_{23} \\ A_{31} & D_3 & A_{33} \end{bmatrix}}{\det \begin{bmatrix} A_{11} & A_{12} & A_{13} \\ A_{21} & A_{22} & A_{23} \\ A_{31} & A_{32} & A_{33} \end{bmatrix}}, \quad (50)$$

$$z_c = \frac{\det \begin{bmatrix} A_{11} & A_{12} & D_1 \\ A_{21} & A_{22} & D_2 \\ A_{31} & A_{32} & D_3 \end{bmatrix}}{\det \begin{bmatrix} A_{11} & A_{12} & A_{13} \\ A_{21} & A_{22} & A_{23} \\ A_{31} & A_{32} & A_{33} \end{bmatrix}}. \quad (51)$$

and,

$$A_{11} = 2(x_2 - x_1), \quad (52)$$

$$A_{12} = 2(y_2 - y_1), \quad (53)$$

$$A_{13} = 2(z_2 - z_1), \quad (54)$$

$$D_1 = x_2^2 - x_1^2 + y_2^2 - y_1^2 + z_2^2 - z_1^2, \quad (55)$$

$$A_{21} = 2(x_3 - x_1), \quad (56)$$

$$A_{22} = 2(y_3 - y_1), \quad (57)$$

$$A_{23} = 2(z_3 - z_1), \quad (58)$$

$$D_2 = x_3^2 - x_1^2 + y_3^2 - y_1^2 + z_3^2 - z_1^2, \quad (59)$$

$$A_{31} = \det \begin{bmatrix} y_1 & z_1 & 1 \\ y_2 & z_2 & 1 \\ y_3 & z_3 & 1 \end{bmatrix}, \quad (60)$$

$$A_{32} = -\det \begin{bmatrix} x_1 & z_1 & 1 \\ x_2 & z_2 & 1 \\ x_3 & z_3 & 1 \end{bmatrix}, \quad (61)$$

$$A_{33} = \det \begin{bmatrix} x_1 & y_1 & 1 \\ x_2 & y_2 & 1 \\ x_3 & y_3 & 1 \end{bmatrix}, \quad (62)$$

$$D_3 = \det \begin{bmatrix} x_1 & y_1 & z_1 \\ x_2 & y_2 & z_2 \\ x_3 & y_3 & z_3 \end{bmatrix}, \quad (63)$$

For a radial pump, the channel radius of curvature,  $R_c$ , can be expressed by a simpler formula [4]:

$$R_c = \frac{1}{\sin \beta} \frac{1}{-\frac{d\beta(r)}{dr} + \frac{1}{r \tan \beta}}. \quad (64)$$

The derivations for the channel radius of curvature and a comparison between results from Equations (48) and (64) for a radial pump can be found in Sun (2002) [4]. The results show a good match between both equations.

**Rotational Speed Effect.** The rotation effect on the friction factor for straight pipes with circular cross-section was studied by Ito (1971) [9].

Ito (1971) suggested that the flow regime and friction factor for rotational pipes were influenced by rotational Reynolds number  $N_{\text{Re}\Omega}$  defined by,

$$N_{\text{Re}\Omega} = \frac{\omega d_H^2 \rho_l}{\mu_l}. \quad (65)$$

If the rotational Reynolds number is less than 28, the pipe can be considered stationary. If the rotational Reynolds number is equal or greater than 28, rotational speed effects must be considered.

**Critical Reynolds Number.** The transition criteria distinguishing laminar and turbulent flow occur at a critical Reynolds number function of the rotational Reynolds number.

$$(N_{Re})_{crit\_rotation} = \begin{cases} 1070(N_{Re\Omega})^{0.23} & \text{if } N_{Re\Omega} \geq 28 \\ 2300 & \text{if } N_{Re\Omega} < 28 \end{cases} \quad (66)$$

*Laminar Flow.* If  $N_{Re} \leq (N_{Re})_{crit\_rotation}$ , then the flow is laminar.

The friction factor for a rotating pipe under laminar flow conditions depends on the dimensionless parameter  $K_{laminar}$  defined as,

$$K_{laminar} = N_{Re\Omega} N_{Re} \quad (67)$$

The following are the expressions of the rotating multiplication factor under laminar flow.

(a) If  $K_{laminar} \leq 220$  and  $\frac{N_{Re\Omega}}{N_{Re}} < 0.5$  then,

$$F_{rotation} = \frac{f_{circular, straight, rotation}}{f_{circular, straight, stationary}} = 1 \quad (68)$$

(b) If  $220 < K_{laminar} < 10^7$  and  $\frac{N_{Re\Omega}}{N_{Re}} < 0.5$  then,

$$F_{rotation} = \frac{f_{circular, straight, rotation}}{f_{circular, straight, stationary}} = 0.0883K_{laminar}^{0.25} (1 + 11.2K_{laminar}^{-0.325}) \quad (69)$$

(c) If  $\frac{N_{Re\Omega}}{N_{Re}} \geq 0.5$  then,

$$F_{rotation} = \frac{f_{circular, straight, rotation}}{f_{circular, straight, stationary}} = \frac{0.0672N_{Re\Omega}^{0.5}}{1 - 2.11N_{Re\Omega}^{-0.5}} \quad (70)$$

*Turbulent Flow.* If  $N_{Re} > (N_{Re})_{crit\_rotation}$ , then the flow is turbulent.

The friction factor for a rotating pipe under turbulent flow conditions depends on the dimensionless parameter  $K_{turbulent}$  defined as,

$$K_{turbulent} = \frac{(N_{Re\Omega})^2}{N_{Re}} \quad (71)$$

The following are the expressions of the rotating multiplication factor under turbulent flow.

(a) If  $K_{turbulent} < 1$  then,

$$F_{rotation} = \frac{f_{circular, straight, rotation}}{f_{circular, straight, stationary}} = 1 \quad (72)$$

(b) If  $1 \leq K_{turbulent} \leq 15$  then,

$$F_{rotation} = \frac{f_{circular, straight, rotation}}{f_{circular, straight, stationary}} = 0.942 + 0.058K_{turbulent}^{0.282} \quad (73)$$

(c) If  $K_{turbulent} > 15$  then,

$$F_{rotation} = \frac{f_{circular, straight, rotation}}{f_{circular, straight, stationary}} = 0.942K_{turbulent}^{0.05} \quad (74)$$

**Calculation of Friction Factor for Impeller and Diffuser Channels.** The equations presented in previous sections enables the determination of the critical Reynolds Number, flow regimes, and friction factor taking into consideration the cross-section shape, curvature and rotational effects once at a time.

In actual ESP, the diffuser channel is subjected to two of those effects simultaneously, whereas the impeller channel is influenced by all three effects. In this way, the flow regime and friction factor in an actual ESP channel should take into consideration a superimposition of those effects.

**Critical Reynolds Number and Flow Regime.** In this study, Critical Reynolds Number with Increment Superimposition is proposed as follows.

The two critical Reynolds numbers under the two simultaneous effects: rectangular and curvature effects in a diffuser have a same value as follows:

$$(N_{Re})_{crit\_effect,diffuser} = (N_{Re})_{crit\_normal} \times \left[ 1 + \left( \frac{(N_{Re})_{crit\_rectangular}}{(N_{Re})_{crit\_normal}} - 1 \right) + \left( \frac{(N_{Re})_{crit\_curved}}{(N_{Re})_{crit\_normal}} - 1 \right) \right] \quad (75)$$

For an impeller, the three critical Reynolds numbers under the three simultaneous effects: rectangular, curvature, and rotational effects in an impeller have a same value as follows:

$$(N_{Re})_{crit\_effect,impeller} = (N_{Re})_{crit\_normal} \times \left[ 1 + \left( \frac{(N_{Re})_{crit\_rectangular}}{(N_{Re})_{crit\_normal}} - 1 \right) + \left( \frac{(N_{Re})_{crit\_curved}}{(N_{Re})_{crit\_normal}} - 1 \right) + \left( \frac{(N_{Re})_{crit\_rotation}}{(N_{Re})_{crit\_normal}} - 1 \right) \right] \quad (76)$$

**Friction Factor.** Superimposition of multiplication factors adopted by Sachdeva (1988) [1, 2] is used in this study. It is assumed that each individual effect multiplication factor can be superimposed to obtain the total friction factor for an

impeller or diffuser. An additional rectangular multiplication factor is included into the new model in this study.

Therefore, the friction factor for an impeller,

$$f_{\text{impeller}} = \frac{F_{\text{rectangular}} F_{\text{curved}} F_{\text{rotation}} f_{\text{circular, straight, stationary}}}{F_{\text{rectangular}} F_{\text{curved}} f_{\text{circular, straight, stationary}}}, \quad (77)$$

and the friction factor for a diffuser,

$$f_{\text{diffuser}} = \frac{F_{\text{rectangular}} F_{\text{curved}} f_{\text{circular, straight, stationary}}}{F_{\text{rectangular}} F_{\text{curved}} f_{\text{circular, straight, stationary}}}. \quad (78)$$

### Boundary Conditions

To solve the pressure distributions along the impeller and diffuser, the boundary conditions of pressure and velocity are needed.

**Pressure Boundary Conditions.** The entrance pressure in an impeller is the starting point when one calculates the pressure distribution along the impeller channel. Assuming no losses between the impeller eye and the impeller entrance and using Bernoulli's equation, one obtains,

$$\frac{P_{\text{impeller\_entrance}} - P_{\text{Eye}}}{\rho_l g} + \frac{V_{\text{impeller\_entrance}}^2 - V_{\text{Eye}}^2}{2g} = 0, \quad (79)$$

where  $V_{\text{impeller\_entrance}}$  is the fluid absolute velocity at the impeller entrance;  $V_{\text{Eye}}$  is the fluid absolute velocity at the impeller eye.  $P_{\text{impeller\_entrance}}$  is the pressure at the impeller entrance;  $P_{\text{Eye}}$  is the pressure at the impeller eye. Then, the impeller entrance pressure can be related to the impeller eye pressure as,

$$P_{\text{impeller\_entrance}} = P_{\text{Eye}} + \frac{\rho_L (V_{\text{Eye}}^2 - V_{\text{impeller\_entrance}}^2)}{2}. \quad (80)$$

After the discharge pressure in the impeller is obtained, one must have the entrance pressure in the diffuser to continue calculating the pressure distribution along the diffuser.

Similarly, the diffuser entrance pressure  $P_{\text{diffuser\_entrance}}$  can be related to the impeller discharge pressure  $P_{\text{impeller\_discharge}}$  as,

$$P_{\text{diffuser\_entrance}} = P_{\text{impeller\_discharge}} - \frac{\rho_L (V_{\text{diffuser\_entrance}}^2 - V_{\text{impeller\_discharge}}^2)}{2}, \quad (81)$$

where  $V_{\text{diffuser\_entrance}}$  is the relative fluid velocity at the diffuser entrance;  $V_{\text{impeller\_discharge}}$  is the absolute fluid velocity at the impeller discharge.

Similarly, the impeller eye pressure at the next stage  $P_{\text{next\_Eye}}$  can be related with the diffuser discharge pressure

$P_{\text{diffuser\_discharge}}$  as,

$$P_{\text{next\_Eye}} = P_{\text{diffuser\_discharge}} + \frac{\rho_L (V_{\text{diffuser\_discharge}}^2 - V_{\text{next\_Eye}}^2)}{2}, \quad (82)$$

where  $V_{\text{diffuser\_discharge}}$  is the fluid absolute velocity at the diffuser discharge;  $V_{\text{next\_Eye}}$  is the fluid absolute velocity at the next stage of the impeller eye, and  $V_{\text{Eye}} = V_{\text{next\_Eye}}$  for single-phase incompressible flow.

**Velocity Boundary Conditions.** In addition to the pressure boundary conditions, the actual flow angles at the impeller entrance and discharge can affect the velocity boundaries. The calculation approach of the actual fluid angles at the impeller entrance and discharge in this study can be found in next section.

### Results

**Input Data.** An example of the input data under single-phase flow is shown in Table 1 and Table 2. The single stage of the pump is shown in Fig.5.

**Comparison between model results and experimental data.** The first step is using water to obtain the actual flow angles at the impeller entrance and discharge by adjusting the two actual flow angles and matching the performance from the frictional model with the performance from the manufacturer at a level near the best efficiency point. The matched pump performances are shown in Fig.2.

In this example, the geometric angles were estimated visually. If the actual geometric angles are given by the manufacturer, then the values in Table 1 and Table 2 can be replaced by the accurate values, and the actual flow angles of the impeller should be adjusted again.

For simplicity in this example, the actual flow angles of the impeller were assumed the same as the impeller's geometric angles, since no accurate impeller geometric angles were available. Finally, the actual flow angles of the impeller were obtained through performance matching as shown in Fig.2. The actual flow angle projection on the plane perpendicular to the axis at impeller discharge was obtained as 23°. The actual flow angle projection on the plane perpendicular to the axis at impeller entrance was obtained as 38°.

In this example, the head difference in the Fig.2 is the shock loss for water at a base rotational speed 50 HZ, which can be regressed as,

$$\Delta h_{\text{shock,base}} = 3.3 \times 10^{-6} Q_l^2 - 5.122 \times 10^{-3} Q_l + 2.042 \quad (83)$$

Therefore, the three coefficients in this example are:

$$a_{shock,base} = 3.3 \times 10^{-6}, \quad b_{shock,base} = -5.122 \times 10^{-3},$$

$$c_{shock,base} = 2.042.$$

**Affinity Law.** The second step is to predict the pump performance for different operation conditions. The predicted pump performance for different rotational speeds for water is shown in Fig.6, which has the almost same value as the pump performance for different rotational speeds from the Affinity Law, using a base of 50 HZ performance.

**Model Capability.** The model is capable of predicting pump performance for different rotational speeds and different liquid properties, such as viscosities under single-phase flow, as shown in Fig.7, which must be verified when the experimental data are available.

### Conclusions

A new one-dimensional single-phase liquid model has been developed for different ESP pump types, liquid properties, and motor rotational speeds.

- A pressure frictionless ODE was derived for an ESP pump. It has been verified through integration and comparison with Euler head equation.
- The model for wall friction factor to account for the three effects was improved. A new equation to decide the critical Reynolds number in ESP is proposed and needs to be verified.
- A new shock loss model including rotational speed has been proposed and verified after comparing the model results with the head performances from manufacturer for different rotational speeds.

### Acknowledgements

The authors would like to thank the technical and financial support of TUALP member companies during the execution of this work. The progress on this research is the result of the support of ENI-AGIP, Centrilift, PDVSA, Pemex, ONGC, Schlumberger, Shell and Total Fina Elf.

### Nomenclature

$a$	=Channel width, m
$b$	=Channel height for impeller or diffuser, m
$d_{eq}$	=Equivalent diameter, m
$d_H$	=Hydraulic diameter, m
$\left(\frac{dp}{dr}\right)_f$	= Pressure radial gradient due to fluid friction, Pa/m
$f$	= Friction factor
$f_B$	= Blasius friction factor for smooth, straight pipes
$F_{curved}$	=Curvature multiplication factor
$F_{rectangular}$	=Multiplication factor of rectangular effect

$g$	=Gravitational acceleration, m/s <sup>2</sup>
$H$	=Channel height, m
$j$	=Indicator for impeller or diffuser, $j=1$ for the impeller and $j=-1$ for the diffuser
$K_{laminar}$	=Dimensionless parameter for a rotating pipe under laminar flow conditions for liquid
$K_{turbulent}$	=Dimensionless parameter for a rotating pipe under turbulent flow conditions for liquid
$l$	=Aspect ratio of the rectangular channel
$n$	=Channel numbers
$N_{Re}$	=Reynolds number
$(N_{Re})_{crit\_curved}$	=Critical Reynolds number for curvature effect
$(N_{Re})_{crit\_normal}$	=Critical Reynolds number for a normal pipe, namely, a straight stationary pipe with circular cross section
$(N_{Re})_{crit\_rectangular}$	=Critical Reynolds number for rectangular effect
$(N_{Re})_{crit\_rotation}$	=Critical Reynolds number for rotational effect
$N_{Re\_eq}$	=Equivalent Reynolds number
$N_{Re}$	=Reynolds Numbers for liquid
$N_{Re\Omega}$	=Rotational Reynolds number
$Q_{bep}$	=Flow rate at the best efficiency point, m <sup>3</sup> /s
$H_{bep}$	=Pump head at the best efficiency point, m
$p$	=Pressure, Pa
$p_{Eye}$	=Impeller eye pressure of the stage intake, Pa
$p_{next\_Eye}$	=Impeller eye pressure of the next stage, Pa
$\Delta p_{shock}$	=Shock loss, Pa
$Q_l$	=Liquid flow rate, m <sup>3</sup> /s
$r$	=Radial position of a point on the impeller, m
$R_c$	=Radius of curvature along a channel, m
$s$	=Distance from the entrance tip of impeller or diffuser to certain location on the streamline, m
$U$	=Peripheral velocity, m/s
$V$	=Absolute flow velocity, m/s
$V_r$	=Radial absolute velocity of fluid, m/s
$V_\theta$	=Peripheral absolute velocity of fluid, m/s
$V_z$	=Axial absolute velocity of fluid, m/s
$W$	=Relative flow velocity between the fluids and the channel, m/s
$x, y, z$	=Cartesian coordinates, m
$x_c, y_c, z_c$	=Center coordinates of the approximate circular interval of the channel, m
$z$	=Axial coordinate from pump intake to discharge, m

**Greek**

$\beta$	=Blade angle, which is the angle between the outward blade tangent and the peripheral line opposing the rotating direction
$\beta_1$	=Entrance blade angle;
$\beta_2$	=Discharge blade angle
$\gamma$	=Angle between the tangent of the blade and the plane perpendicular to the axis
$\Delta p_{shock,base}$	=Shock loss at base rotational speed, Pa
$\Delta p_{stage}$	=Pressure increment per stage, Pa
$\varepsilon$	=Absolute roughness of the channel, m
$\theta$	=Tangential angle coordinate
$\mu_l$	=Liquid viscosity, Pa.s
$\rho_l$	=Liquid Density, kg/m <sup>3</sup>
$\omega$	=Angular velocity of impeller or diffuser, rad/s
$\omega_{impeller}$	=Angular velocity of the rotating shaft or of the impeller, rad/s

**Subscripts**

$1$	=Entrance
$2$	=Discharge
$1,2,3$	=Any three points along the channel
$bep$	=Best efficiency point
$c$	=Center of a circle
$curvature$	=channel curvature, “straight” or “curved”
$effect$	=“rectangular”, “curved”, or “rotational”
$eq$	=Equivalent
$Eye$	=Impeller eye
$f$	=Friction
$H$	=Hydraulic
$l$	=Liquid
$laminar$	=Laminar flow
$movement$	=Channel movement, “stationary” or “rotation”
$next$	=Next
$r$	=Radial
$s$	=Stream line
$shape$	=cross section shape, “rectangular” or “circular”
$shock$	=Shock loss

$turbulent$	=Turbulent flow
$v$	=Vertical
$z$	=Axial from pump intake to pump discharge
$\theta$	=Tangential
$\Omega$	=Rotational

**REFERENCES**

1. Sachdeva, R., Doty, D.R. and Schmidt, Z.: *Two-Phase Flow through Electric Submersible Pumps*, Ph.D. Dissertation, the University of Tulsa, Oklahoma (1988).
2. Sachdeva, R., Doty, D.R. and Schmidt, Z.: “Performance of Electric Submersible Pumps in Gassy Wells,” *SPE Production & Facilities* (February 1994).
3. Cooper, P. and Bosch, H.: “Three Dimensional Analysis of Inducer Fluid Flow,” NASA Report CR-54836, TRW ER-6673A, February 1966.
4. Sun, D. and Prado, M.G.: *Modeling Gas-Liquid Head Performance of Electric Submersible Pumps*, Ph.D. Dissertation, the University of Tulsa, Oklahoma (2002).
5. Stepanoff, A.J.: *Centrifugal and Axial Flow Pumps*, John Wiley & Sons, Inc. (1957).
6. Minemura, K., Uchiyama, T., Shoda, S. and Kazuyuki, E.: “Prediction of Air-Water Two-Phase Flow Performance of a Centrifugal Pump Based on One-Dimensional Two-Fluid Model,” *Journal of Fluids Engineering*, Vol. **120** (June 1998).
7. Churchill, S.W., “Friction-Factor Equation Spans All Fluid-Flow Regimes”, *Chemical Engineering*, Nov. 1977.
8. Schlichting, H., *Boundary Layer Theory*, Translated by J. Kestin, Pergamon Press, London, England (1955) pp 427.
9. Ito, H. and Nanbu, K.: “Flow in Rotating Straight Pipes of Circular Cross Section,” *J. Basic Eng.*, Trans., ASME (September 1971).
10. Shah, R.K.: “A Correlation for Laminar Hydrodynamics Entry Length Solutions for Circular and Noncircular Ducts,” *J. Fluids Eng.*, Vol. **100** (1978) pp 177-179.
11. Jones, O.C.: “An Improvement in the Calculation of Turbulent Friction in Rectangular Ducts,” *J. Fluids Eng.*, Vol. **98**, (1976) pp 173-180.
12. Cornish, R.J., “Flow in a pipe of Rectangular Cross Section,” *Proceedings of the Royal Society*, **120(A)**, London, 1928, pp.691-700.
13. Ito, H.: “Friction Factors for Turbulent Flow in Curved Pipes,” *J. Basic Eng.*, Trans., ASME (June 1959).
14. Bird, R.B *et al.*: *Transport Phenomenon*, John Wiley & Sons, New York City (1960).
15. Blevins, R. D.: *Applied Fluid Dynamics Handbook*, Krieger Publishing Company, Malabar, Florida (1992).
16. Chen, X. and Zhao Z.: *Investigation of the Three-Dimensional Flow in the Centrifugal Impeller and Its Performance Analysis*, MS Thesis (in Chinese), Chongqing University, China (May 2000).
17. Harun, A.F., Prado, M.G. and Shirazi, S.A. and Doty, D.R.: “Two-Phase Flow Modeling of Inducers,” Proceedings of the ASME/OMAE Joint ETCE 2000 Conference, New Orleans, Louisiana (14-17 February 2000).
18. Hydraulic Institute: *Hydraulic Institute Standards for Centrifugal, Rotary & Reciprocating Pumps*, 14<sup>th</sup> Edition (1983)
19. Wiesner, F.J.: “A Review of Slip Factors for Centrifugal Impellers”, *Journal of Engineering for Power*, October 1967, Transaction of the ASME.

**Table 1 – Input Data for the Impeller and Liquid Properties**

Angular velocity	2915 rpm
Shaft outer radius	0.007 m
Impeller Entrance radius	0.029 m
Impeller Discharge radius	0.048 m
Liquid Density	1000 kg/m <sup>3</sup>
Liquid Viscosity	1e-3 Pa.s
Channel Wall Roughness	1e-4 m

**Table 2 – Input Geometric Data for the Impeller and Diffuser**

Data	Impeller	Diffuser
$\beta_{h\_entrance}$	38°	10°
$\beta_{h\_discharge}$	23°	85°
$\gamma_{entrance}$	0°	30°
$\gamma_{discharge}$	0°	80°
Number of Channels	7	8
Channel Height	0.01 m	0.01 m

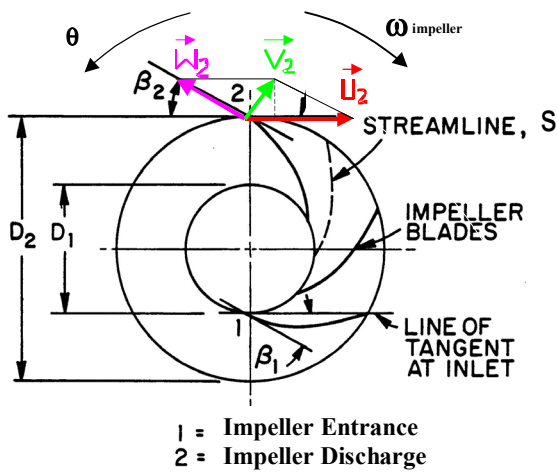


Figure 1 – Sketch of a radial impeller's geometry

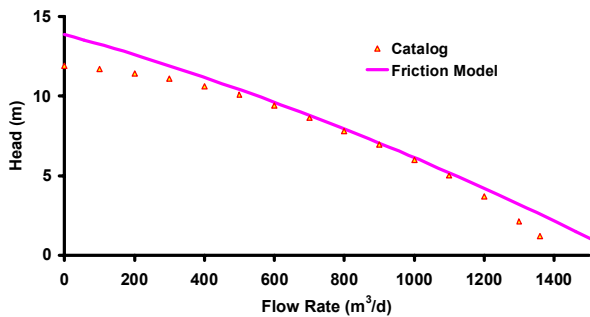


Figure 2 – The Matched Frictional Model Curve and Catalog Curve at the Best Efficiency Point

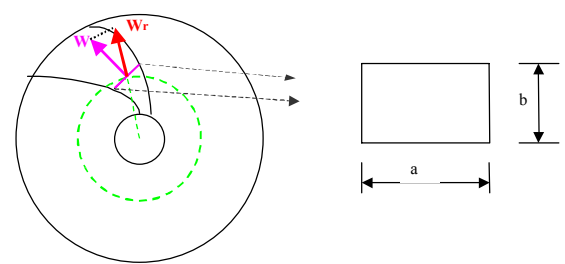


Figure 3 – The shape of A Channel Cross Section

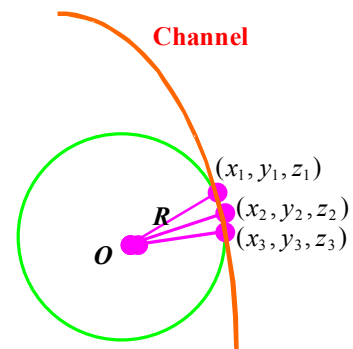


Figure 4 – Radius of Curvature along a Three-Dimensional Channel



Figure 5 – A Pump Stage of the Pump

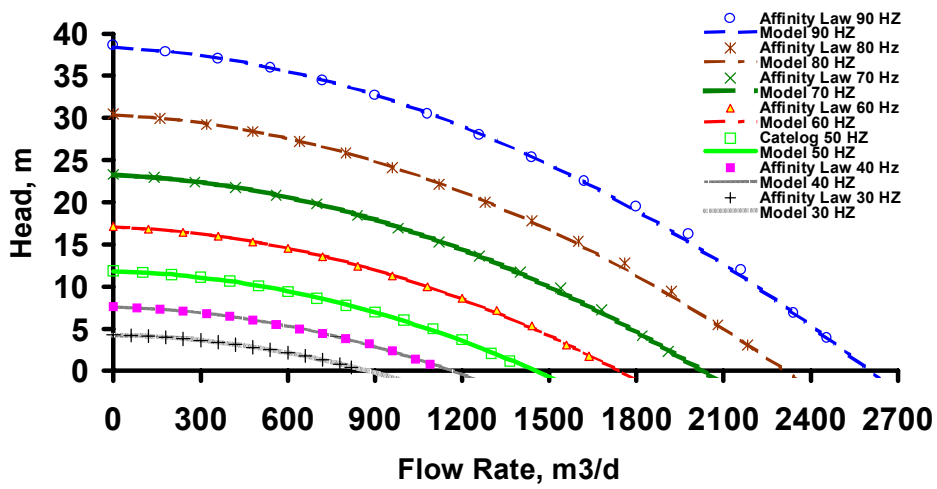


Figure 6 - Pump Performance for different Rotational Speed for Water

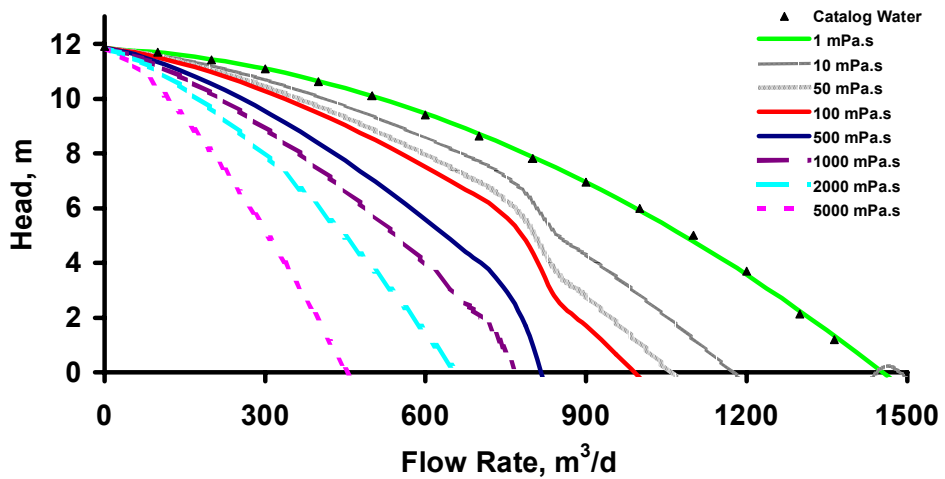


Figure 7 - Viscous Effects from Model under Single-Phase Flow